doi: 10.56761/EFRE2022.R4-O-039201

# Defect-related luminescence in $KLuP_2O_7$ doped with $Pr^{3+}$ ions after irradiation with fast electrons and neutrons

*S.A. Kiselev[1,*], V.A. Pustovarov[1], M.O. Petrova[2], D.A. Tavrunov[1]*

[1]*Ural Federal University, Yekaterinburg, Russia*
[2]*Joint Institute for Nuclear Research, Dubna, Russia*
[*]*s.a.kiselev@urfu.ru*

**Abstract.** This paper reports the spectroscopic properties of praseodymium-doped phosphate, $KLuP_2O_7$ doped with $Pr^{3+}$ ions. Spectra of photoluminescence (PL) upon selective UV photon excitation and PL excitation spectra were measured. Recordings of luminescence spectra were done with pure samples and after irradiating with fast electrons ($E$ = 10 MeV) using the UELR-10-10C2 linear electron accelerator in Ural Federal University and fast neutrons ($E$ > 1 MeV) using IBR-2 reactor in Joint Institute for Nuclear Research. Pure samples demonstrate three typical channels of emission: interconfigurational *d–f* transitions, intraconfigurational *f–f* transitions and defect-related luminescence. After irradiating, significant changes of emission characteristics were observed: redistribution of interconfigurational transitions intensity and growth of defect-related luminescence bands. Several peaks are associated with phosphorus formations in crystal lattice.

**Keywords:** phosphates, $4f^{1}5d^{1}\rightarrow 4f^{2}$ radiative transitions, energy transfer, defect-related luminescence, electron beam irradiation, point defects, defects radiation formation.

## 1. Introduction

Investigation of new scintillating materials pay a lot of attention to rare earth-doped inorganic compound due to potential variety of their applications in different spheres, such as detecting systems, medical tomography, nuclear physics, etc. Praseodymium, a d-element from 6th group of Mendeleev table, produces valence electrons from outer 6*s* level and inner 5*d*. Most properties of rare-earth ions emission are determined by intra- and interconfigurational transitions. Emission transitions 5*d*–4*f* of $Pr^{3+}$ appear when strong enough crystal field moves the lowest $4f^{1}5d^{1}$ excited state lower than $^1S_0$ state [1]. Three types of emission are observed in inorganic scintillators doped with $Pr^{3+}$ ions: interconfigurational *d–f* transitions located in the UV range (250–320 nm), intraconfigurational *f–f* transitions (lines in the visible spectral range) and defect-related luminescence [2, 3]. Cerium ions are in favor for industry, but praseodymium has shorter decay time, and its emission is located at shorter wavelengths. In comparison with impurity $Ce^{3+}$ ions, praseodymium emission is located in higher energy region and has shorter lifetime (20–30 ns instead of 30–60) [4–9].

Optical and electrophysical properties modifying with fluxes of high-level particles is not so common research object due to the theory of electrons, e.g., influence on solids. In most cases, such interactions cause only negative effects, such as decreasing light output, significant structural changes, changing of solids types, etc. But authors supposed to find the way of positive properties modifying. Studied samples – $KLuP_2O_7$ with $Pr^{3+}$-impurity ions have already been approved as potential convenient scintillators with appropriate emission levels of 250–300 nm fast *d–f* transitions with average lifetime of 15–20 ns [10]. So, electron beam and neutron flux irradiation were supposed to be one of the mechanisms to improve optical properties of these samples. Besides influence on intraconfigurational transitions, the main irradiation effect is forming of point defects inside crystal lattice. These defects form a competitive channel for energy transfer from impurity ions. Sustainable defects may act as scintillating channels ready to be used in detecting systems.

The object of the experiment is to research defects existence and their role in optical properties of studied samples after electron irradiation. In general, electrons are able to interact with crystal lattice of solid states in three variants of scenario: deceleration, scattering and absorption. These processes are described with various mechanisms of elastic and inelastic collisions. From defects point of view, ionization of electron shells of the crystal and elastic collisions of fast particles with

nucleus of lattice atoms could be a reason of point defects radiation formation. In case of less electron energy electron fluxes would not be able to transport energy enough for defects formation, so their interaction will be described with phonon generation or with elastic scattering mechanism resulting in changing electron trajectory.

It has to be mentioned that irradiation in common case will increase conductivity of the solid due to generating of additional charge carriers pairs. This condition should not be considered as important as these additional charge carriers would recombine in some period of time. This period depends on the location of carriers – if electron-hole pair are located "not far" from one another, recombination process has high probability to occur. In other cases, recombination would be performed later after diffusion of carriers inside the sample.

## 2. Objects and experiment details

Polycrystalline samples of $Pr^{3+}$-doped $KLuP_2O_7$ were synthesized using a solid state reaction and XRD verified for phase purity at the Laboratory of Luminescent Materials, University of Verona (Italy). Powder microcrystalline material has a stoichiometry of $KLu_{0.99}Pr_{0.01}P_2O_7$ (*i.e.* containing 1 mol.% $Pr^{3+}$ substituting for $Lu^{3+}$). The constituent high purity raw materials $KNO_3$, $(NH_4)_2HPO_4$, $Lu_2O_3$, and $Pr_6O_{11}$ (the last two reagents 4N) were mixed and heat treated in a horizontal furnace in air for 1 h at 400 ºC and 24 h at 750 ºC with intermediate regrinding. The phase purity of the prepared sample was examined using powder X-ray diffraction (PXRD) technique with a Thermo ARL X'TRA powder diffractometer, operating in the Bragg–Brentano geometry and equipped with a Cu anode X–ray source ($K\alpha$, $\lambda$=1.5418 Å) with a Peltier Si(Li) cooled solid–state detector. The obtained PXRD pattern was fully compatible with ICDD Card No. 01–076–7386 [10, 11]. The crystal structure of $KLuP_2O_7$ offers only one site for $Lu^{3+}$ (or $Pr^{3+}$) with a coordination number of 6 and point symmetry $C_1$.

The experimental results presented in this paper were obtained applying different techniques. Photoluminescence (PL) and PL excitation spectra upon excitation in the UV energy range (from 3.5 to 5.8 eV) were measured at room temperature at the Laboratory of Solid State Physics, Ural Federal University. To excite the luminescence a 400 W deuterium lamp and a LOMO DMR-4 primary prismatic double monochromator were used. A secondary DMR-4 monochromator equipped with a Hamamatsu R6358-10 photomultiplier (PMT) was used to detect the emission signal.

In addition, photoluminescence (PL) and PL excitation (PLE) spectra upon excitation in near UV and visible energy ranges (from 230 to 550 nm) were measured at temperature range of 5–310 K using HORIBA iXR320 spectrometer (reverse linear dispersion 2.3 nm/mm) with a cooled CCD camera and ozone-free Xe-lamp. The PL excitation spectra were corrected to the same number of exciting photons using the photodiode included in this spectrometer. A closed-cycle cryogenic cryostat (Cryo Trade Engineering, Moscow) with RDK-20502 Cold Head (Japan) were used for low temperature measurements. A semiconductor diode with Lake Shore controller was used to control and adjust the temperature of the samples. Recordings of luminescence spectra were done with pure samples and after irradiating with fast electrons and fast neutrons.

Electron irradiation was performed at UELR-10-10C2 linear electron accelerator in Ural Federal University. To avoid heating of crystal structure under radiation beam, an existing conveyor system with partial irradiation doses of 11 kGy by fast electrons ($E$ = 10 MeV) was used [12]. Using this system, samples were irradiated during 4 s, then they moved through conveyor circle for approx. 30 mins. Absorbed dose was controlled with film dosimeters. Induced optical density was measured at 550 nm wavelength. Attested film dosimeter SO PDE-1/50 "VNIIFTRI" (for absorbed dose 1–50 kGy region) was used. Measurements have been performed for 15 and 30 cycles. Though dosimeter measurements declare 11 kGy per cycle, calculations with Bethe formula and Kanaya-

Okayama [13] experimental expression for linear energy losses and maximum mileage present value of absorbed dose 4.3 kGy per cycle.

Neutron irradiation was performed at the IBR-2 reactor in Joint Institute for Nuclear Research, Dubna. Density measurements of fast neutrons ($E$ > 1 MeV) were performed with neutron activation analysis (NAA) method with nickel satellite. To carry out NAA with high accuracy, Canberra GC10021 laboratory γ-spectrometer and multichannel analyzer Lynx were used. Flux density amounted $3 \cdot 10^5$ $(cm^2/s)^{-1}$, fluence was $7 \cdot 10^{10}$ $cm^{-2}$. The absorbed dose was determined using FWT-60-00 radiochromic dosimeters containing a leuco dye pararosaniline cyanide in a nylon matrix and an FWT-92D photometer from Far West Technology, Inc. [14].

Decay kinetics of pulsed cathode luminescence (PCL) were measured at the Laboratory of Solid State Physics, Ural Federal University. A small–sized MIRA-2D electron accelerator ($E$ = 120 keV, $\tau_{pulse}$ ~ 25 ns) was used as an excitation source. Luminescence registration is carried out through a double prism monochromator DMR–4 with a photoelectronic multiplier R6358–10. The kinetics of luminescence is displayed on the monitor of the Tektronix color digital oscilloscope TDS–2002 connected with PC.

All emission spectra were corrected for the spectral sensitivity of the detection systems. PL excitation spectra were corrected for wavelength dependent photon flux variation using yellow lumogen.

## 3. Results and discussion

Results of PL measurements are presented at Figs.1–2. Fig.1 contains data about pure and irradiated with electrons samples recorded at room temperature. It can be well observed, that irradiation causes significant changes in emission intensity. The wide UV emission bands dominating in the PL spectra correspond to the parity-allowed interconfigurational radiative transitions from the lowest excited $4f^1 5d^1$ state to multiplets of the ground $4f^2$ electronic configuration of the $Pr^{3+}$ ion. No *f–f* emission lines are observed. Defect-related luminescence is presented by a wide emission band spread from 350 to 600 nm with maximum near 450 nm. With irradiation one can easily determine the redistribution of interconfigurational transitions. Both peaks become equal in intensity.

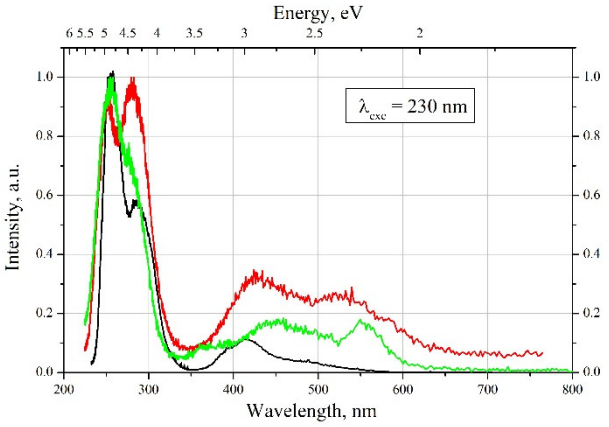


Fig.1. PL spectra of $KLuP_2O_7:Pr^{3+}$ upon UV excitation ($\lambda_{exc}$), $T$ = 295 K before (black) and after irradiation with 10 MeV electrons from LINAC (red – 15 cycles, green – 30 cycles).

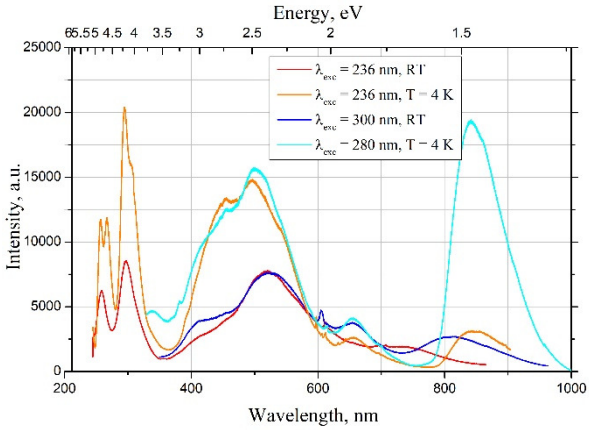


Fig.2. PL spectra of $KLuP_2O_7:Pr^{3+}$ upon UV excitation ($\lambda_{exc}$), $T$ = 5 and 295 K before (red, blue) and after irradiation with neutrons (orange, cyan).

The wide band in 400–600 nm region is supposed to be produced by defect-related luminescence. Pure samples present a low-intensity one-peak band with maximum at 415 nm. Irradiation causes a remarkable growth of intensity in this region. Moreover, both types of irradiation (as it will be shown

later) lead to appearance of new maxima in 540, 650 and 840 nm regions. Moreover, as it can be observed, value of absorbed dose affects the intensity of defect-related luminescence. The bigger the dose the higher will be the intensity.

When the crystal lattice interacts with heavy ions flux, arriving particles would cause cascade of atoms offsets inside of lattice. Electrons with energy more than 1 MeV as well as fast neutrons would generate point defects along distribution trajectory. Most of appearing defects would be stable, during lifetime they are able to diffuse deeper in material and recombine with interstitial atoms if such interaction is energy-allowed. The more is the energy of particles the deeper they can enter the material and form the defect. Most probably, appearing defects would be Frenkel defects as atoms will be moved out from their crystal lattice nodes. So, while irradiating the samples we suppose to observe two mechanisms of radiation formation of point defects: impact mechanism – elastic collisions of fast particles with nucleus of lattice atoms, and ionization mechanism – excitation of electron shells of the crystal and their ionization. As studied samples are phosphates, other measurements not published yet demonstrate similar defect-related luminescence behavior, so one can suppose that defects are partly formed by phosphorus, oxygen atoms and their combinations. These radicals form complex defects acting as big available centers for capturing arriving electrons. In contrast with single ions, this electron will be captured not by one ion, but by set of oxygen ions, forming axial symmetry of appearing center.

Fig.2 presents the results of PL spectra measurements for samples, irradiated with neutron fluxes at room temperature and $T = 5$ K. For both types of excitation – 236 nm (5.2 eV) and 300 nm (4.2 eV) intensity of defect-related luminescence rises. Also, it should be mentioned that four main bands are observed: 440 nm (2.82 eV), 520 nm (2.38 eV), 650 nm (1.91 eV) and 840 nm (1.48 eV). From cyan-colored PL spectra in Fig.2 (280 nm excitation wavelength, $T = 5$ K) is well seen that though first three bands are excited with practically equal efficiency, 840 nm band reaches the intensity of interconfigurational transitions at low temperatures.

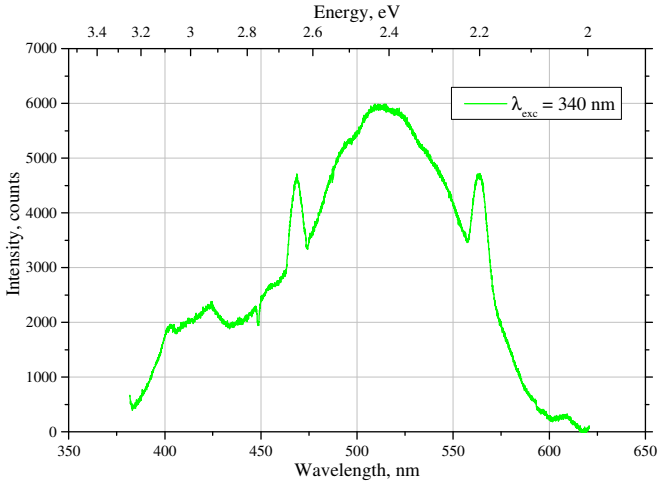


Fig.3. PL spectrum of $KLuP_2O_7:Pr^{3+}$ upon UV excitation ($E_{exc}$), $T = 5$ K after irradiation with neutrons.

Presented in Fig.3 PL spectrum demonstrates a complex structure of defect-related emission band. At least 4–5 component can be included for analyzing. More detailed research of these bands is supposed to be performed in future. The fact that can be cooperated with information of defects emission given in Refs. [15, 16] is that asymmetric band with maximum at 420–430 nm corresponds to $PO_2$ defects. This point defect with declared emission lifetime of 5–6 ms can be most efficient excited with 4.7 and 6.4 eV.

Few words about intraconfigurational $4f^2$–$4f^2$ transitions should be added. As it can be concluded, the output of intraconfigurational emission is rather low in comparison with *d–f* transitions. Such situation is typical for compounds, which Stokes shift of interconfigurational transitions does not exceed 0.4 eV [1]. As was previously calculated in Ref. [10], for $KLuP_2O_7:Pr^{3+}$ *d–f* Stokes shift does not exceed 0.38 eV. Nevertheless, at Fig.2 one can observe a group *f–f* transitions corresponding to praseodymium ions, terminated at $^1D_2$. Most visible are 596 nm ($^1D_2$–$^3H_4$) and 612 nm ($^1D_2$—$^3H_5$).

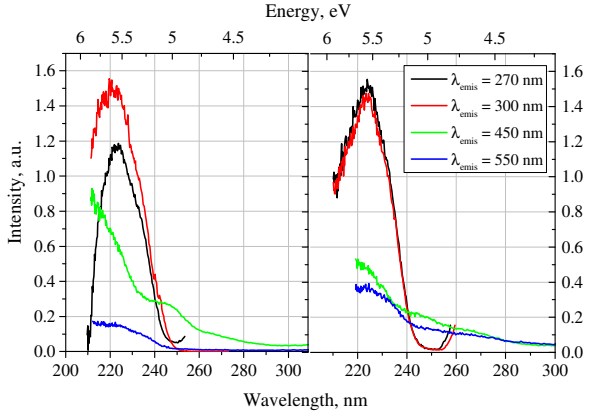


Fig.4. PL excitation spectra of $KLuP_2O_7:Pr^{3+}$ of emission bands ($\lambda_{emis}$), $T$ = 295 K before (left) and after irradiation with electrons (right).

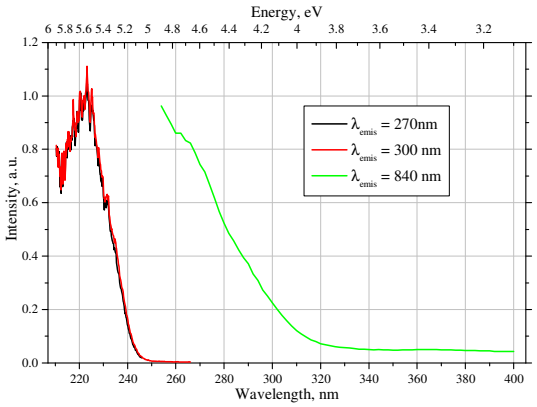


Fig.5. PL excitation spectra of $KLuP_2O_7:Pr^{3+}$ of defect-related luminescence emission bands ($E_{emis}$), $T$ = 5 K after irradiation with neutrons.

PL excitation spectra recorded monitoring different emission bands ($\lambda_{emis}$) are presented in the Fig.4 and Fig.5. Excitation features related to intracenter $Pr^{3+}$ $4f^15d^1$–$4f^2$ transitions are observed as a wide complex band in the UV region between 200 and 250 nm. PL excitation spectrum recorded for the emission band located at 450 nm demonstrates a weak feature near 5 eV that is followed by a further increase of the excitation efficiency while scanning the spectrum towards upper energy limit of 6 eV. PL excitation spectra (Fig.4) demonstrate the most effective excitation at 5.5 eV. These spectra indicate that we observe not direct excitation of defects, but efficient energy transport from impurity centers to defects of crystal lattice. Irradiation of crystal structure leads to breaking of atom bonds with radical groups. Stable hole radical $(PO_4)^{2-}$ forming band of 520 nm emission is generated. Moreover, excitation bands of this defect is common with excitation of interconfigurational transitions. Emission band 840 nm is characterized with 4.7 eV excitation. According to Ref. [15], defect group $PO_2$ is well excited with 4.7 and 6.4 eV. Further investigation with higher excitation energies is needed.

Fig. 6 demonstrate temperature quenching of defect-related luminescence. The PL yield is nearly independent of temperature in the range of 5–20 K. At $T$ = 300 K the PL yield drops to about 0.15 of the initial value. The dependence was satisfactory fitted using the Mott-Seitz activation-energy model

$$I(T) = \frac{I_0}{\left(1 + A \cdot \exp\left(\frac{-\varepsilon_a}{k_B \cdot T}\right)\right)}, \quad (1)$$

as illustrated by the solid line in Fig.6, Inset. Here, $A$ is a constant, $k_B$ is the Boltzmann coefficient and $\varepsilon_a$ is the thermal activation energy. The fitting suggests that this quantity for the observed thermal quenching process is about $\varepsilon_a$ ~ 0.035 eV. Another parameter that is often used to describe the temperature quenching is a characteristic quenching temperature $T_Q$ which corresponds to the temperature at which the quantum yield decreases by 50% assuming a 100% quantum yield at low

temperatures. As follows from the results presented in Fig.6, the characteristic quenching temperature for defect-related emission in $KLuP_2O_7:Pr^{3+}$ is $T_Q$ = 140 K.

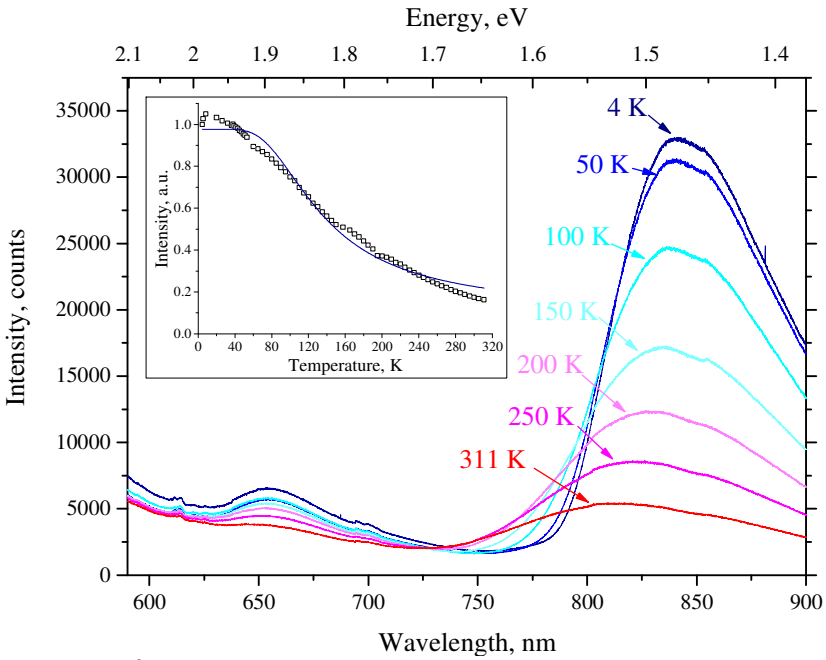


Fig.6. PL spectra of $KLuP_2O_7:Pr^{3+}$ irradiated with neutrons upon UV excitation ($\lambda_{exc}$ = 280 nm) measured at different temperatures. Inset: Temperature dependance of 840 nm emission band.

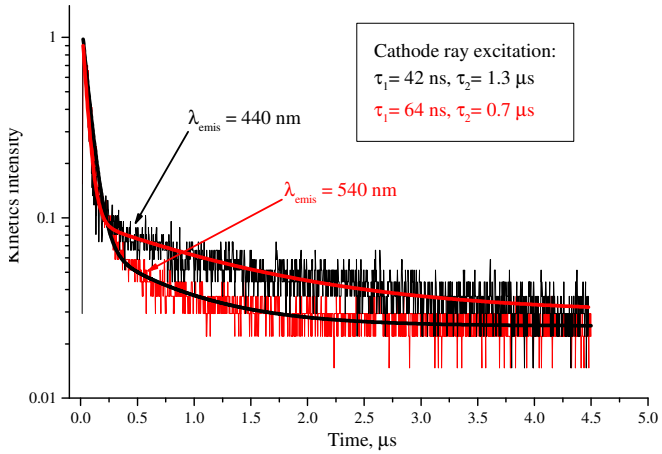


Fig.7. PCL decay kinetics recorded monitoring defect-related emission of $KLuP_2O_7:Pr^{3+}$, $T$ = 295 K. Solid lines demonstrate fitting curves obtained using Eq. (2).

PCL decay curves of $KLuP_2O_7:Pr^{3+}$ are presented in Fig.5. For better understanding it must be underlined that luminescence decay kinetics curves in most cases are well fitted with multiexponential approximation (2):

$$I(t) = \sum A_i \cdot \exp\left(-\frac{t}{\tau_i}\right) + I_0, \qquad (2)$$

Here, $I_0$ is the contribution of background level describing the role of slow components. $A_i$ has to amount the amplitude maximum of each exponential component with $\tau_i$ as lifetime. Both decay curves of 440 and 540 nm emission lines are well fitted with the two-exponential approximation. The

440 nm line is characterized with parameters of $\tau_1 \sim 42$ ns and $\tau_2 \sim 1.3$ μs, while contribution of slow component is $10^{-1}$. The 550 nm line can be fitted with $\tau_1 \sim 64$ ns and $\tau_2 \sim 0.7$ μs, while contribution of slow component reaches $5 \cdot 10^{-2}$. To produce the whole description, previously observed $Pr^{3+}$ $4f^1 5d^1 \rightarrow 4f^2$ emission lifetimes of the main decay component are $\tau = 18$–$20$ ns [10].

## 4. Conclusion

In summary, set of spectra of studied $KLuP_2O_7:Pr^{3+}$ is measured and discussed. PL spectra of pure samples are dominated with fast $Pr^{3+}$ interconfigurational $4f^1 5d^1$–$4f^2$ radiative transitions. Due to a small Stokes shift, the contribution of $4f^2$–$4f^2$ intraconfigurational transitions is very low. Samples were irradiated with electrons ($E$ = 10 MeV) from linear electron accelerator and fast neutrons ($E$ > 1 MeV) from IBR-2 reactor. After irradiation, significant changes in emission spectra behaviour are found.

First, one can observe redistribution of interconfigurational transitions intensity. Second, contribution of defect-related luminescence in total light output drastically rises. Thus, it can be easily concluded that irradiation with electrons and neutrons act as efficient way of forming defects. Most common, we observe both mechanisms of Frenkel defect formation – impact collisions and ionization. While comparing obtained results with other studied samples, one can find near-similar behaviour of defect-related emission bands. As other studied samples were also phosphates, it was supposed that appearing defects are phosphorus-related. Obtained in [15, 16] data about such structures allows to declare that observed defects are $(PO_4)^{2-}$ and $PO_2$ radical groups. They act as competitive channel of energy transfer from impurity ions.

Luminescence decay kinetics recorded monitoring the $Pr^{3+}$ defect-related emission pulsed cathode excitation was found to demonstrate a multi-exponential behavior described with two main components ($\tau_1 \sim 42$ ns, $\tau_2 \sim 1.3$ μs and $\tau_1 \sim 64$ ns, $\tau_2 \sim 0.7$ μs). The presence of slow component is due to manifestation of delayed energy transfer processes. As PL excitation spectra demonstrate, defects luminescence can be either caused with band-to-band or selective excitation. The light output of UV-excited $Pr^{3+}$ defect-related luminescence is nearly stable in temperature range of 5–40 K, then shows a pronounced drop and can be described with quenching temperature of $T_Q$ = 140 K. The corresponding thermal quenching is characterized by an activation energy of about $\varepsilon_a \sim 0.035$ eV.

Further investigation of optical properties management is supposed to be performed both increasing absorbed dose got by electron beam irradiation and after interacting with neutron fluxes. Obtained results for two values of absorbed dose with electron irradiation demonstrate direct dependance between emission intensity and length of irradiation. Phosphorous groups are supposed to demonstrate a significant susceptibility towards this type of irradiation.

## Acknowledgements

The work was partially supported by the Ministry of Science and Higher Education of the Russian Federation through the basic part of the government mandate, project No. FEUZ-2020-0060. Authors also appreciate assistance and want to thank M. Bettinelli and F. Piccinelli (University of Verona, Italy) for submitting certified samples for these primary studies.

## 5. References

[1] Srivastava A.M., *J. Lumin.*, **169**, 445, 2016; doi: 10.1016/j.jlumin.2015.07.001
[2] Gorbenko V., Zych E., Voznyak T., Nizankovskiy S., Zorenko T., Zorenko Yu., *Opt. Mater.*, **66**, 271, 2017; doi: 10.1016/j.optmat.2017.02.00
[3] Kristianpoller N., Weiss D., Khaidukov N., Makhov V.N., Chen R., *Rad. Meas.*, **43**(2), 245, 2008; doi: 10.1016/j.radmeas.2007.11.001
[4] Nikl M., Laguta V.V., Vedda A., *Phys. Status Solidi (b)*, **245**, 1701, 2008; doi: 10.1002/pssb.200844039

[5] Nikl M., Ogino H., Yoshikawa A., Mihokova E., Pejchal J., Beitlerova A., Novoselov A., Fukuda T., *Chem. Phys. Lett*., **410**, 218, 2005; doi: 10.1016/j.cplett.2005.04.115
[6] Carrasco I., Bartosiewicz K., Piccinelli F., Nikl M., Bettinelli M., *J. Lumin*., **189**, 113, 2017; doi: 10.1016/j.jlumin.2016.08.022
[7] Pustovarov V.A., Razumov A.N., Vyprintsev D.I., *Phys. Solid State*, **56**, 347, 2014; doi: 10.1134/S1063783414020267
[8] Wisniewski D., Wojtowicz A.J., Drozdowski W., Farmer J.M., Boatner L.A., *J. Alloy Compd*., **380**, 191, 2004; doi: 10.1016/j.jallcom.2004.03.042
[9] Zych A., de Lange M., Donega C. d. M., Meijerink A., *J. Appl. Phys*., **112**, 013536, 2012; doi: 10.1063/1.4731735
[10] Pustovarov V.A., Ivanovskikh K.V., Kiselev S.A., Trofimova E.S., Omelkov S., Bettinelli M., *Opt. Mat*., **108**, 110234, 2020; doi: 10.1016/j.optmat.2020.110234
[11] Trevisani M., Ivanovskikh K., Piccinelli F., Bettinelli M., *Zeitschrift fur Naturforschung B*, **69**, 205, 2014; doi: 10.5560/znb.2014-3260
[12] Maslovskaya A.G., Ilika S.N., Sivunov A.V., *Series: Nat. Econ. Sci*., **51**, 2010; URL: cyberleninka.ru/article/n/modelirovanie-elektronnyhtraektoriy-v-tverdyh-telah-metodom-monte-karlo
[13] Kiryakov A.N., Zyryanov S.S., Kortov V.S., *Proc. Sec. Int. Youth Sci. Conf. «Physics. Technologies. Innovations. PTI-2015»*, *Ekaterinburg, Russia*, 232, 2015; url: hdl.handle.net/10995/87901
[14] Petrova M.O., Bulavin M.V., Rogov A.D., Yskakov A., Galushko A.V., *Instrum. Exp. Tech.*, **65**, 371, 2022; doi: 10.1134/S0020441222030046
[15] Girard S., et al., Rev. Phys., **4**, 100032, 2019; doi: 10.1016/j.revip.2019.100032
[16] Origlio G., Messina F., Cannas M., Boscaino R., Girard S., Boukenter A., Ouerdane Y., *Phys. Rev. B*, **80**, 205208, 2009; doi: 10.1103/PhysRevB.80.205208